Solid State Ionics 52 (1992) 3–13
North-Holland

SOLID
STATE
IONICS

Considerations in design and characterization of solid-state electrochemical systems

Meilin Liu and Ashok Khandkar
Ceramatec, Inc., 2425 South 900 West, Salt Lake City, UT 84119, USA

The performance of a solid-state electrochemical system depends critically on the transport process in the bulk phases as well as the mass transfer and charge transfer across interfaces. The bulk transport process, such as diffusion under a chemical potential gradient and migration under an electric field, is relatively well-understood and properly characterized. The phenomena occurring at an interface, however, have received little attention due either to the lack of understanding of these processes or to the experimental difficulty with determination of the interfacial properties. Although interfacial phenomena are far more complex in nature than bulk transport processes, their effect on the system performance is becoming more and more important, particularly for systems involving thin-film electrolytes or for operation at low temperatures. In both cases, the kinetics of interfacial processes dominate the performance characteristics. This paper addresses considerations in analysis and characterization of interfacial phenomena in solid-state electrochemical systems. The physical significance and characteristics of these processes are demonstrated in solid oxide fuel cells, oxygen sensors, and thermoelectric generators based on solid electrolytes. Furthermore, approaches to improve the interfacial properties and to optimize system performance are also illustrated.

1. Introduction

Solid electrolytes have found wide applications in energy storage and conversion, gas separation, electrosynthesis, sensing of chemical species, and other electrochemical processes [1]. For instance, chemical sensors based on solid electrolytes have been widely used in monitoring various molecules (such as O_2, CO, NO_x, etc.) in gas streams, ionic species (Na^+, Ca^{2+}, etc.) in aqueous solutions or in molten salts or glass, and metal constituents (Na, Si, Ca, etc.) in molten metals or alloys.

In electrochemical systems involving liquid electrolytes, mass transport in the bulk phase or near the interface of the liquid electrolyte can be accurately controlled by hydrodynamic methods such as rotating electrodes [2]. In addition, the overpotential across an interface can be readily monitored or measured by positioning a Luggin capillary reference electrode to minimize ohmic drop contributions. In a solid-state electrochemical system, however, the transport process is less controllable and the investigation of electrode kinetics at the interface of such a system is frequently complicated by the corresponding mass transfer to or away from the interface and by ohmic drop contributions.

Recently, experimental isolation in performance of each individual cell component (anode, cathode, electrolyte, current collector, and interconnect materials) has been successfully accomplished in our laboratory through unique test cell design, proper positioning of reference electrodes, together with appropriate electrochemical techniques, such as 4-probe impedance spectroscopy, the current-interruption method, potential sweep techniques, and galvanostatic testing.

The purpose of this paper is to emphasize the existence of interfacial resistance, the impact of interfacial phenomena on the performance of various solid-state electrochemical systems, and the methodology and procedures for characterization of such a system, including cell design, selection of experimental conditions, and application of characterization techniques. In addition, these principles will be illustrated in the study of electrode kinetics and in investigation of characteristic performance of solid oxide fuel cells.

2. Interfacial phenomena

2.1. Significance of interfacial phenomena

The processes occuring at an interface, including adsorption–desorption, chemical reaction, surface diffusion, charge transfer, and mass transfer processes, play a very important role in many solid-state electrochemical systems.

In a potentiometric *sensor*, it is frequently observed that poor interfacial contact or slow electrode kinetics considerably delay the sensor response and develop potential errors [3]. In addition, it is the selectivity of the catalytic materials at the surface which greatly influences the selectivity, sensitivity, speed of response, reproducibility, and hence precision and accuracy of the sensing device.

In a system incorporating current flow, such as a *fuel cell*, an *oxygen pump*, or a *thermoelectric generator*, on the other hand, electrode polarization often contributes significantly to the loss of efficiency and severely reduces the power output or productivity.

In *electrosynthesis*, such as partial oxidation of methane, the efficiency and productivity depend critically on the catalytic activity of the interface where the desired products or intermediate species are favorably produced.

Furthermore, trends in solid-state electrochemical devices emphasize microfabricated thin-film devices and systems operated at low temperatures. Clearly, interfacial phenomena become more important as the thickness of the electrolyte is reduced and as the operating temperature is lowered.

2.2. Existence of interfacial resistance

Although interfacial phenomena are critical to many electrochemical systems, the kinetics of interfacial processes has been traditionally assumed to be sufficiently fast so that the interfacial resistance was typically ignored in the analysis of a *solid-state* electrochemical system. The existence of an interfacial resistance is, in fact, evident from many impedance spectroscopy studies, polarization measurements, potential sweep measurements, as well as I–V characteristics of many solid-state ionic devices.

Shown in fig. 1 are some typical impedance spectra of automobile oxygen sensors based on yttria-stabilized zirconia (YSZ) and platinum electrodes. Since these impedance data were obtained from a two-electrode configuration, the intercept of the impedance locus with the real axis at high frequencies corresponds to the resistance of the electrolyte, either the total resistance of the electrolyte (when the grain boundary resistance is negligible) or the resistance to bulk transport through grains (when the grain boundary resistance is significant). The spectra indicate that, although the impedances of the electrolytes are relatively constant, the impedances of the interfaces varied dramatically from sensor to sensor, illustrating the effect of electrode processing on the interfacial impedance. Two observations can be made from the spectra: (1) the interfacial impedance dominates the overall impedance of the sensor at low temperatures, and (2) the interfacial impedance depends critically on the manner in which the platinum was applied to the electrolyte, i.e. the processing of the electrode. In addition, these sensors behaved very differently in performance; the sensors with higher impedance exhibited much slower response and more potential deviation from the expected Nernst potential, particularly at low temperatures.

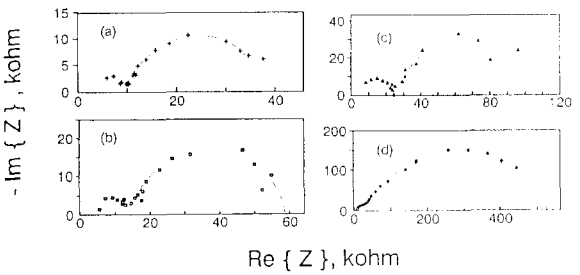

Fig. 1. Impedance spectra of (automobile) oxygen sensors based on yttria-stabilized zirconia (YSZ) with platinum electrodes at 350 °C in air. The sensing electrodes were prepared in the following manner: (a) thermal decomposition of $PtCl_4$ on a rough surface of YSZ, (b) thermal decomposition of $PtCl_4$ on an untreated surface (as sintered), (c) painting and firing of platinum slurry, and (d) sputtering of platinum.

Fig. 2 shows some typical impedance spectra of the interfaces between YSZ and three different electrode materials exposed to air at 1000 °C. Each impedance spectrum was obtained from a three-electrode configuration and the depressed semicircles correspond to the processes occuring at a single interface. These spectra clearly indicate that the interfacial imped-

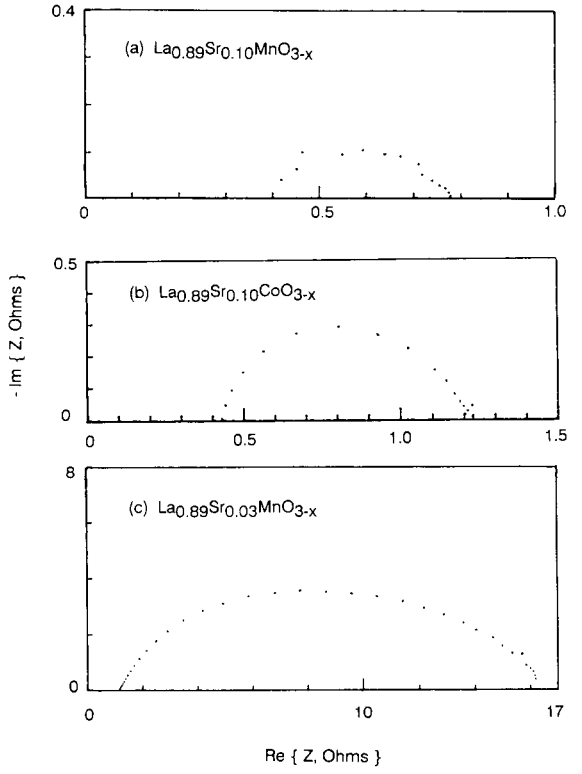

Fig. 2. Impedance spectra of the cathode–electrolyte interfaces of solid oxide fuel cells at 1000 °C in air. The electrolyte was YSZ and the electrodes were (a) $La_{0.89}Sr_{0.1}MnO_{3-x}$, (b) $La_{0.89}Co_{0.1}MnO_{3-x}$, and (c) $La_{0.89}Sr_{0.03}MnO_{3-x}$. The impedances were measured on cells as showing in fig. 7 with electrode area of 25 cm^2.

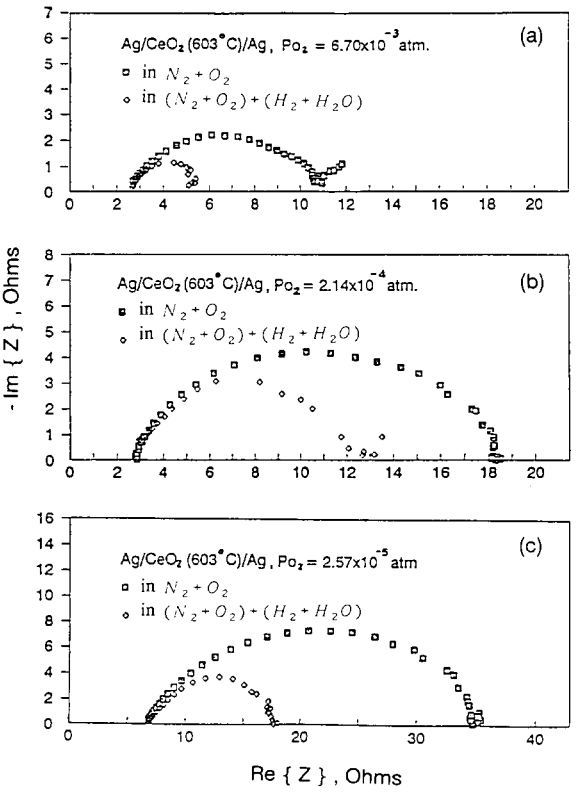

Fig. 3. Impedance spectra of oxygen heat engines at 603°C in three different partial pressures of oxygen: (a) $P_{O_2}=6.7\times10^{-3}$ atm, (b) $P_{O_2}=2.14\times10^{-4}$ atm, (c) $P_{O_2}=2.57\times10^{-5}$ atm. The electrolyte was calcia-doped ceria and the electrodes were silver.

ance, or the catalytic activity of the interface, is a strong function of the composition or stoichiometry of electrode materials. Among the three materials evaluated, $La_{0.89}Sr_{0.10}MnO_{3-x}$ exhibited the highest catalytic activity for oxygen reduction and evolution.

Shown in fig. 3 are some typical impedance spectra of a thermoelectric generator based on oxygen-anion conductors. The impedances were measured across tabular cells with $(CeO_2)_{0.85}(CaO)_{0.15}$ electrolyte and silver electrodes exposed to a mixture of N_2 and O_2 or to a mixture of N_2, O_2, H_2O and H_2. These spectra clearly illustrate the effect of the atmosphere on the interfacial impedance of the device. It is evident from the spectra that the interfacial impedance increases with the decrease in partial pressure of oxygen whereas it decreases when a supporting medium, a mixture of H_2O and H_2, was introduced into the system.

Fig. 4 shows the impedance spectra of an oxygen sensor based on YSZ electrolyte and platinum electrode at three different temperatures. Clearly, the impedance of the interface increased much faster than the impedance of the bulk electrolyte as the temperature was reduced, indicating that the activation energy for interfacial transport process is much greater than that for the bulk transport within the electrolyte. As a result, the interfacial impedance becomes more significant at low temperatures.

Shown in fig. 5 is a typical cyclic voltammogram of an LSM/YSZ interface in a O_2 concentration cell. The non-linear behavior clearly indicates that the interfacial resistance contributes to the overall cell impedance. In addition, it is worth noting that the

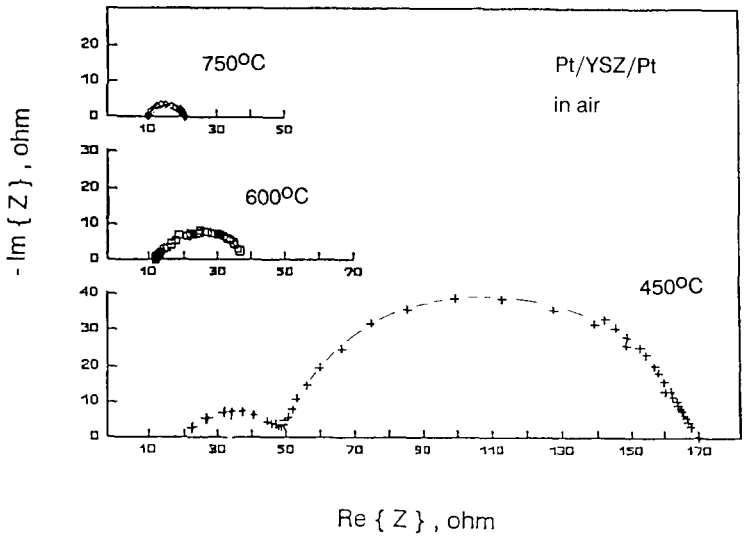

Fig. 4. Impedance spectra of a tubular oxygen sensor in air at different temperatures. The electrolyte was YSZ and platinum was used as electrode.

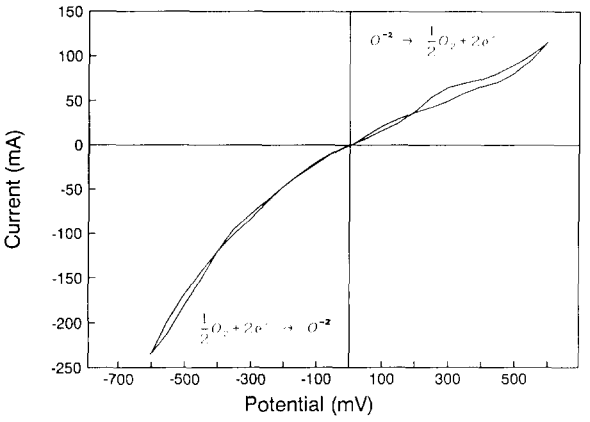

Fig. 5. A typical cyclic voltammogram of an LSM/YSZ interface at 900 °C in air. The potential sweep rate was 20 mV s^{-1}.

cathodic process is faster than the anodic process under the testing conditions.

2.3. Interfacial degradation

It is a common observation that degradation in performance of electrochemical systems frequently originated from interfacial phenomena, such as chemical reactions, physical mixing or interdiffusion [4], microstructural changes (sintering), mismatch in thermal expansion [5], impurity contamination, electrochemical degradation, physical delamination, and other unrecognized processes.

Shown in fig. 6 are the impedance spectra of three oxygen sensors under similar operating conditions. First of all, the impedances of the interfaces are a strong function of the formulation of the platinum slurries. Secondly, the resistances of the interfaces increased significantly while the resistances of the bulk electrolytes stayed relatively constant during continuous operation. Characterization of sensor performance indicates that the increase in interfacial impedance led to slower sensor response. In addition, the sensor with electrode of Pt-02 degraded much faster than the sensors with the other two platinum electrodes (Pt-01 and Pt-03).

Furthermore, chemical reactions between the electrolyte and electrode materials during processing also cause deterioration in system performance [6].

3. Methodology

The operation of a solid-state electrochemical system, in general, involves mass transport through bulk phases as well as mass and charge transfer across interfaces. Accordingly, the overall response of a cell

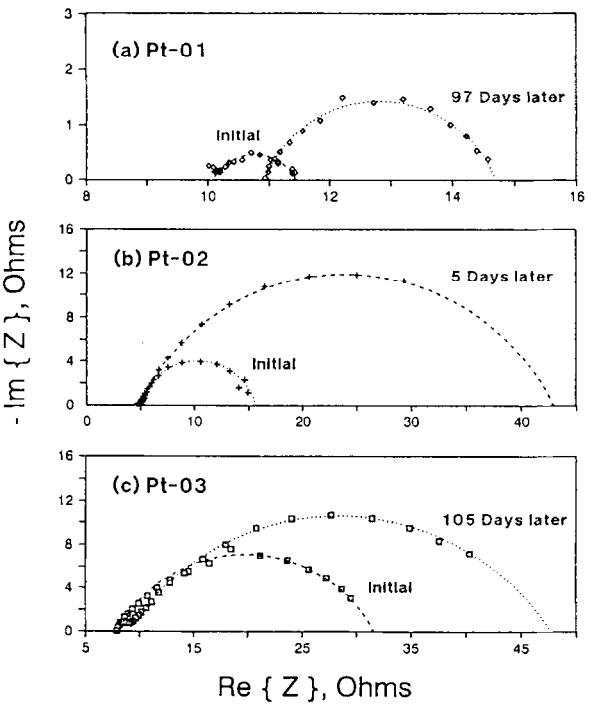

Fig. 6. Impedance spectra of oxygen sensors at 750 °C in air. The electrolyte was YSZ and three types of platinum pastes (Pt-01, Pt-02 and Pt-03) were used as electrodes.

under certain experimental or operational conditions typically reflects the complexity of these transport processes in the system and it is very difficult to extrapolate useful information about each individual process. Outlined below is a general procedure for analysis of a solid-state electrochemical system.

3.1. Experimental design

The primary objective of experimental design is to isolate the performance of response of each component of an electrochemical cell under investigation, including electrolyte, electrode, interconnect, current collector, as well as the interfaces between them.

The experimental design can be accomplished through (i) appropriate cell design (ii) selection of suitable experimental conditions, and (iii) application of proper characterization techniques. The testing cell has to be so designed that each cell components can be monitored individually. Experimental conditions, on the other hand, should be so chosen that the process to be studied can be emphasized, mathematical description of the process is simple, physical interpretation of the process is unique, and implications of the observations are fruitful. Characterization techniques should be able to distinguish the response of a single component from the response of the overall system.

Successful isolation of each cell component and reliable characterization of each individual process is crucially important to the identification of the limiting factor to the performance of a cell and hence to the effective improvement of cell performance.

3.2. Identification of critical process or component

A critical process (or component) is the process (or component) which contributes the most to the overall impedance of a system and hence limits the performance of the system. Once an appropriate experimental design is identified, each and every cell component, interface or process has to be investigated individually. The confidence in determination of the response of each process or component can be validated by matching the sum of the individual response of each process with the overall response of the system. Comparison of the impedance of each component or process under various operational conditions will give valuable information on which components or process is the critical process or the rate-limiting step.

3.3. Understanding of the critical process or component

Once a process or a component is identified as the rate-limiting step for the overall process, a logical step forward is to understand the detailed mechanism of the process in order to improve the system performance most effectively.

If, for instance, the electrode kinetics is rate-limiting to the system performance, the kinetic details, including reaction pathway, reaction mechanism, and kinetics parameters, have to be investigated to achieve electrocatalysis. The electrode kinetics may further involve adsorption–desorption, surface diffusion, and electron transfer processes. If the charge

transfer step is rate-limiting while the other steps are relatively fast, one has to speed up the electron transfer process. On the other hand, if the surface diffusion of electroactive species from an adsorption site to a reaction site limits the overall process, minimization of the surface diffusion path would effectively improve the electrode kinetics. Furthermore, the microstructure of the electrode materials and the interface also play a very important role in the electrode kinetics. The effects of the processing procedures and microstructure on the interfacial processes should be investigated as well.

If, on the other hand, the bulk transport within the electrolyte is rate-limiting to the overall process, the transport mechanism has to be clarified so that a possible approach to achieve high conductivity can be proposed. If the conductivity cannot be improved considerably, however, reducing the thickness of the electrolyte could effectively reduce the impedance of the electrolyte.

If other physical contact is rate-limiting, then better processing techniques should be sought to improve the contact of the interface.

4. Experimental

4.1. Cell design for separation of cell component

The design of a *single cell* will emphasize the isolation of the response of each component whereas the design of a *system* (e.g. a device with multi-layer stacking) will stress the isolation of the performance of each cell or component.

Shown in fig. 7 is one of the cell configurations used routinely to separate the performance of the electrolyte, the anode–electrolyte interface, and the cathode–electrolyte interface [7]. It is important, however, to be aware of the existence of an ohmic resistance between a working electrode (a cathode or an anode) and a reference electrode, due to the physical gap between them. The ohmic resistances between each pair of electrodes for a given cell can be readily determined by impedance spectroscopy or the current-interruption method.

Electrochemical cells used for mechanistic studies include specially-designed fuel cells (O_2/YSZ/H_2), oxygen concentration cells (O_2/YSZ/O_2), and cells

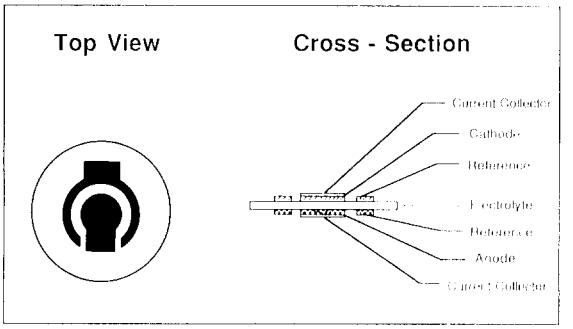

Fig. 7. A schematic view of a test cell used for performance isolation of each cell component.

incorporating interconnect materials. Similar cell configurations were also used to isolate the performance of the interconnect materials, the anode–interconnect interface, cathode–interconnect interface, and the bonding materials between two cell components.

4.2. Materials

Solid oxide fuel cell: Tape-cast yttria-stabilized zirconia (YSZ, 8 mol% Y_2O_3) was used as electrolyte throughout the study. The electrode materials evaluated in this study include modified $La_{(1-x)}Sr_xMnO_3$(LSM) and $La_{(1-x)}Sr_xCoO_3$-(LSCo) for oxygen reduction and nickel-based (Ni/ZrO_2) electrodes for fuel oxidation. A slurry of electrode materials was screen printed on the electrolyte discs and subsequently fired at high temperatures (1150–1350 °C).

Oxygen sensors: Zirconia-based materials, such as $(ZrO_2)_{92}(Y_2O_3)_8$ and $(ZrO_2)_{92}(Y_2O_3)_4(Yb_2O_3)_4$, were used as solid electrolyte for oxygen sensors. The electrode materials evaluated in this study include noble metals, mixed-conductive oxides, and composite materials. A slurry of electrode materials was brush painted onto electrolyte tubes or screen-printed onto discs. The sensors used for stability studies were operated at 750 °C with a continuous flow of sample gases.

Thermoelectric generators: Electrolyte materials used for oxygen heat engines include zirconia-based and ceria-based materials. Electrode materials studied for this application include perovskites (LSM, LSCo, etc.), precious metals (Pt and Ag), and silver

alloys. The partial pressure of oxygen was controlled either by an electrochemical oxygen pump based on YSZ or by introduction of a H_2/H_2O mixture into the system [8].

Current collector: The electronic conductivity of electrode materials can dramatically influence the uniformity of potential and current distribution on the electrodes. When the electronic conductivity of an electrode material is inadequate, a current collector with sufficient electronic conductivity should be used to ensure that the current and potential are distributed uniformly throughout the working electrode. In general, non-uniform distribution will complicate experimental observation and the interpretation of the results. Platinum or silver, either in the form of mesh or porous layer, was used as current collector throughout the study.

4.3. Electroanalytical techniques

Unless otherwise stated, a perturbation input signal was always applied to a whole cell while the response was monitored across only a single interface or a single cell component with the appropriate positioning of two reference electrodes. Thus, the observed response (impedance, overpotential, etc.) observed depends only on a single component or interface rather than on the overall cell. Accordingly, the complications associated with multi-interface or multi-time-constant processes were effectively minimized or eliminated and the interpretation of experimental results was dramatically simplified.

Four-probe impedance spectroscopy has been successfully employed to investigate the processes occurring at electrode–electrolyte interfaces, to elucidate the reaction mechanism, to determine the kinetic parameters, and also to identify effective catalysts for oxygen reduction and evolution. Solartron 1255 (frequency response analyzer) and 1286 (electrochemical interface) impedance analysis systems, interfaced with an IBM PC/386, were used to measure the impedance of solid-state electrochemical cells in the frequency range from mHz to MHz.

The ohmic resistance of a single interface was validated using *current-interruption* techniques. In addition, the potential decay in a current-interruption experiment also carries valuable information on the electrode kinetics [9]. The step-current signals, generated by a Galvanostat (Solartron 1286), were applied to a cell under test while the corresponding potential response during current interruption was monitored and recorded using a Tektronix 50 MHz storage oscilloscope.

Potential (or current) sweep or step methods were further used to confirm the current-interruption and impedance measurements. The I–V characteristics of fuel cells were determined using galvanostatic, potentiostatic, and load testing methods. Two types of potentiostat/galvanostat (Princeton Applied Research EG&G 273 and Solartron 1286) were used to control the potential or current with a three- or four-electrode configuration.

Experimental error brought about by inappropriate cell design and characterization techniques often has a considerable impact on data interpretation. For instance, investigation of electrode kinetics using large-amplitude controlled-current or controlled-potential techniques typically introduce error due to mass transport limitations or ohmic drop across the working electrode and the reference electrode [10]. The effect of mass transport on the kinetics can be eliminated effectively by perturbation techniques, such as impedance spectroscopy, whereas the ohmic polarization has to be compensated accordingly. The IR compensation usually involves the determination of the ohmic resistance of an interface using impedance spectroscopy or current-interruption technique. Shown in fig. 8 is a typical potential

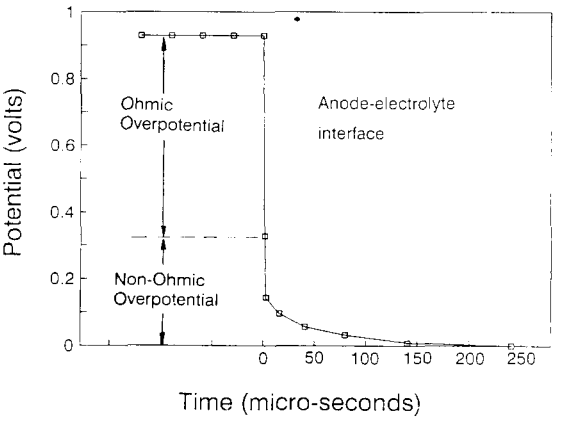

Fig. 8. Potential response in a current-interruption measurement at the anode–electrolyte interface of a fuel cell: H_2 with 3% H_2O, $Ni/YSZ/La_{0.89}Sr_{0.1}MnO_{3-x}$, air at 1000 °C. (The electrode area was 2.5 cm^2; the applied steady state current was 1.0 Å.)

response after a steady current was interrupted. The ohmic resistance of a component or an interface can be uniquely determined.

5. Illustrative examples

5.1. Performance isolation of cell components

Some typical impedance spectra of a Ni/YSZ/LSM cell at 1000 °C are shown in fig. 9. Spectrum (a) is the total impedance of the cell, which was obtained from a two-electrode configuration. This spectrum represents two or more processes occurring simultaneously in the cell during the measurement. Clearly, the intercept of the locus with the real axis at high frequencies corresponds to the impedance of the electrolyte, the resistance to transport of O^{2-} across the grains of the electrolyte (since the grain boundary resistance is negligible at 1000 °C). Difficulties associated with the interpretation of the rest of the spectrum, however, include determining how many processes contributed to the total impedance as well as identifying which physical process corresponds to which specific portion of the spectrum. The electrochemical processes accountable for the total impedance include oxygen reduction at the cathode–electrolyte interface and hydrogen oxidation at the anode–electrolyte interface. In addition, the electrode reactions, both oxygen reduction and hydrogen oxidation, could involve more than one step, each step having its own characteristic time constant. Perhaps the most confusing situation in interpretation of impedance data is the case of overlapping of processes with similar time constants.

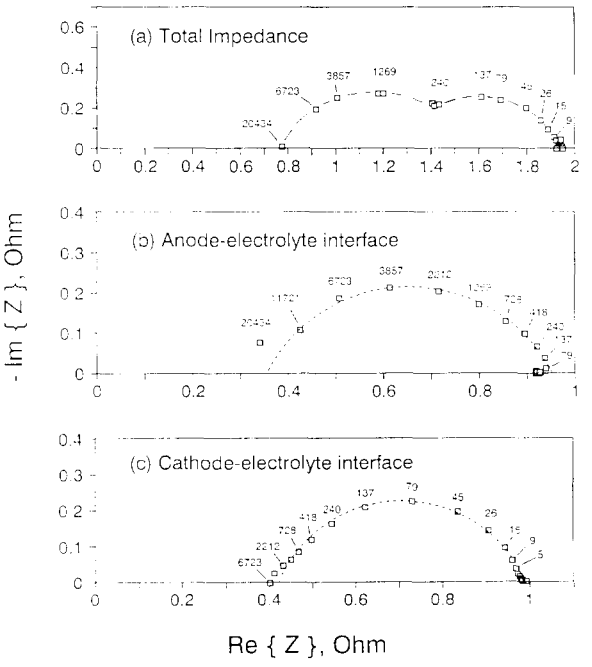

Fig. 9. Impedance spectra of a cell (H_2 with 3% H_2O, Ni/YSZ/$La_{0.89}Sr_{0.1}MnO_{3-x}$, air) at 1000 °C: (a) the total impedance of the cell, (b) the impedance of the anode–electrolyte interface, and (c) the impedance of the cathode–electrolyte interface. The numbers by the data points represent the frequency in Hertz. The working electrode area was 2.5 cm^2.

With two additional reference electrodes, however, the impedance of the interface between anode and electrolyte or between cathode and electrolyte was obtained, as shown in fig. 9 (b) and (c), respectively. The interpretation of these impedance spectra is straightforward. In spectrum (b), for instance, the intercept of the impedance locus with the real axis at high frequencies corresponds to the ohmic resistance between the anode and the reference electrode, due to the physical gap between the two electrodes, while the depressed semicircle represents the interfacial processes occurring at the interface, from which the charge transfer resistance for hydrogen oxidation can be readily determined. Similarly, the ohmic resistance between the cathode and the reference electrode and the charge transfer resistance for oxygen reduction can be determined from spectrum (c).

5.2. Identification of limiting factors to cell performance

Shown in fig. 10 is a summary of the performance of each cell component and the overall cell. The total potential loss was split into three parts, the potential drop across the electrolyte (*IR* drop), the anodic overpotential (across the anode–electrolyte interface), and the cathodic overpotential (across the cathode–electrolyte interface). For this specific cell, the ohmic drop across the electrolyte clearly contributes most to the overall polarization loss at high operating current (above 500 mA). In this case, improvement in electrolyte conductivity will most ef-

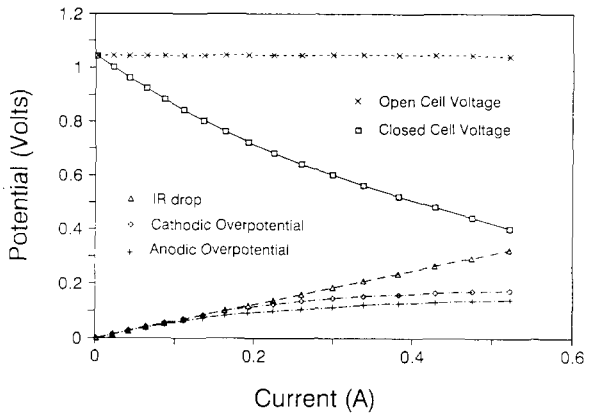

Fig. 10. Current–potential characteristics of a fuel cell. The total overpotential of the cell at various operating currents was divided into three contributions: the *IR* drop across the electrolyte, the anodic overpotential, and the cathodic overpotential.

fectively improve the overall cell performance. At low operating current (below 100 mA), however, each cell component makes similar contribution to the overall polarization loss. Therefore, the successful separation in performance of each cell component clearly identifies the rate-limiting factor to a specific cell or process and hence provides valuable information for most effective improvement of the cell performance.

5.3. *Understanding the critical processes*

In this section, investigation of electrode kinetics for oxygen reduction and evolution will be taken as an example. Understanding of the reaction pathway and reaction mechanism will provide valuable information for achieving electrocatalysis.

The overall reaction for oxygen reduction and evolution in a solid-state electrochemical system can be generally described as

$$\tfrac{1}{2}O_2(g) + V_O^{\cdot\cdot} + 2e^- = O_O^{\times} .$$

This reaction is typically accomplished in a number of elemental steps, depending on the nature of the electrode, the electrolyte and the interface, as well as the operating conditions. For instance, at the interface between an electronic conductor (electrode) and an ionic conductor (electrolyte), the reduction of an oxygen molecule to oxygen anions involves at least four elemental steps: (1) adsorption of gas oxygen molecules at the interface, (2) dissociation of the adsorbed oxygen molecules into oxygen atoms, (3) surface diffusion of the oxygen atoms from the adsorption sites to the triple phase points or boundaries, and (4) reduction of the oxygen atoms to oxygen anions. Furthermore, the last step, charge transfer, could consist of two consecutive steps, each involving a single electron transfer.

When a mixed conductor is used as electrode material, there are two clear advantages. First of all, the electrochemically active sites increase from a one-dimensional line to a two-dimensional surface, which has been recognized in the literature [11]. Secondly, the overall reaction involves no surface diffusion of adsorbed oxygen atoms or molecules because all adsorption sites are triple phase boundaries as well, where adsorption , dissociation and reduction can proceed simultaneously. Thus, at the interface between a mixed conductor (electrode) and an ionic or mixed conductor (electrolyte), the reduction of oxygen involves fewer elemental steps.

Analysis [12] indicates that the dependence of the exchange current density on partial pressure of oxygen can be expressed as

$$j_0 \propto P_{O_2}^{1/2}$$

if the adsorption–desorption or dissociation–recombination step is rate-limiting, and

$$j_0 \propto P_{O_2}^{1/4}$$

if the charge-transfer step is rate-limiting.

The impedance spectra of an LSM/YSZ interface are shown in fig. 11. Similar impedance data were also obtained at different temperatures. An immediate observation is that both the Nyquist and the Bode plots clearly indicated that the electrochemical process occurring at the interface was predominantly a one-time-constant process. Again, the intercepts of the impedance locus with the real axis at high frequencies in the Nyquist plot represent the ohmic resistance between the cathode and the reference electrode, which is not of interest in this study. The analysis of these impedance data is entirely focused on the interpretation of the depressed semicircles, which carry valuable information on the electrode kinetics. The charge transfer resistance of the interface was estimated directly from the spectra.

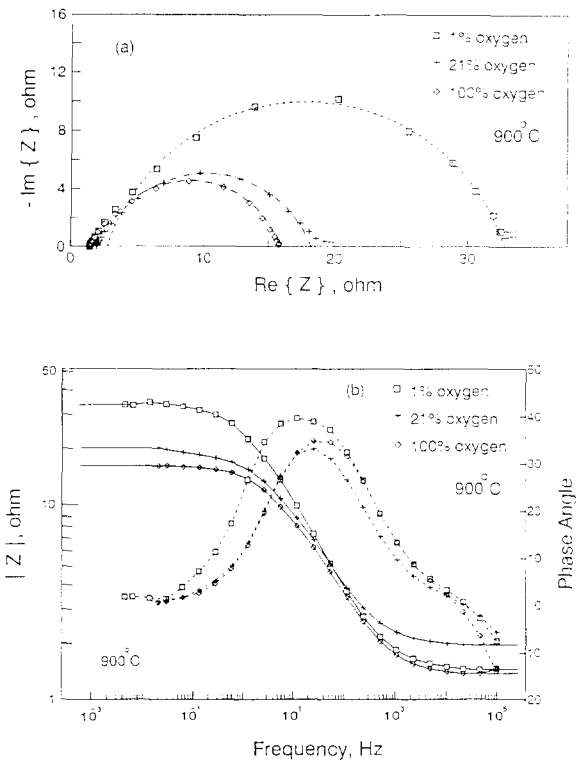

Fig. 11. (a) Nyquist and (b) Bode presentation of the impedance spectra of a single interface: $La_{0.89}Sr_{0.1}MnO_{3-x}$ (LSM)/$(Y_3O_2)_{0.08}(ZrO_2)_{0.92}$ (YSZ). The working electrode area was 2.5 cm^2.

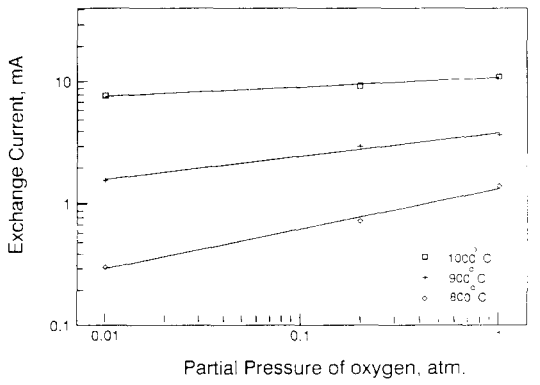

Fig. 12. Dependence of the exchange currents on the oxygen partial pressure (determined from impedance spectra similar to fig. 11).

The calculated exchange currents are shown in fig. 12 as a function of the oxygen partial pressure. The slopes of these linear plots are in the neighborhood of 0.25, suggesting that the rate-determining step in the oxygen reduction/evolution process is the charge transfer step while the adsorption/desorption of oxygen molecules and the dissociation of the adsorbed oxygen molecules are at equilibrium.

The dependence of exchange currents on temperature is shown in fig. 13. It appears that the activation energies varied slightly with the partial pressure of oxygen. This is probably because the catalytic activity of LSM depends on the partial pressure of oxygen as well.

Alternatively, Tafel polarization measurements at a single interface, as shown in fig. 14, give the exchange currents directly. Analysis of these data indicate that the exchange currents determined from impedance spectroscopy closely match the values determined from polarization measurements.

6. Summary and conclusions

The existence of interfacial resistance and its effect on the performance of a solid-state electrochemical system has been demonstrated in oxygen sensors, thermoelectric generators, and solid oxide fuel cells. Even at 1000 °C, the interfacial resistances in a cell of Ni/YSZ/LSM are still significant. In addition, the degradation of an electrochemical system frequently originates from the interfaces. Accord-

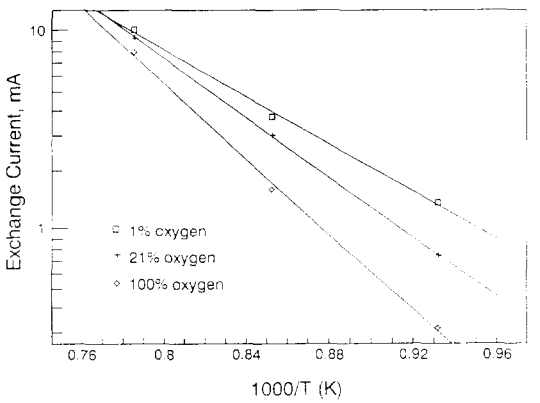

Fig. 13. Dependence of the activation energies for electrode kinetics on the oxygen partial pressure (determined from impedance spectra similar to fig. 11).

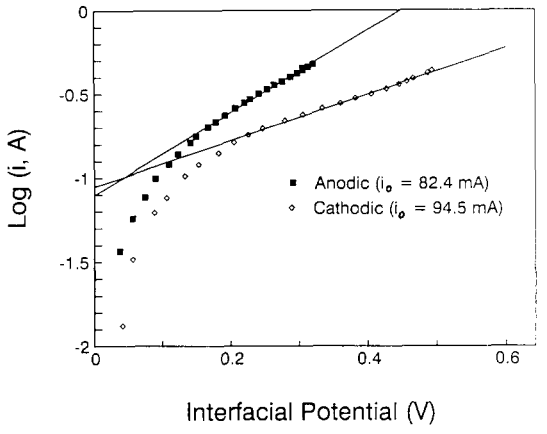

Fig. 14. Tafel polarization measurements of a cathode–electrolyte interface and an anode–electrolyte interface. (The measurements were made on a three-electrode cell with YSZ as electrolyte, $La_{0.89}Sr_{0.1}MnO_{3-x}$ as cathode and Ni as anode.)

ingly, the interfacial phenomena and interfacial resistance have to be taken into consideration in analysis of a solid-state electrochemical system [13,14].

Successful isolation of the performance of each cell component is critical to a fundamental understanding of the individual processes occurring in a solid-state electrochemical system, such as the electrode kinetics or transport processes. Careful identification of the critical component or critical process, which contributes the most to the cell impedance under given conditions, will locate the critical problem in a system, indicating where attention should be focused. A detailed understanding of the mechanism of the critical process in a system will furnish valuable information on effective improvement of the process and hence of the overall performance.

Appropriate cell design, experimental conditions, and characterization techniques have been introduced and demonstrated in solid-state electrochemical systems to achieve isolation in performance of cell components, identification of critical processes, investigation of critical steps, and effective improvement of system performance.

Acknowledgements

The authors gratefully acknowledge Professor Anil Virkar for valuable discussions. The authors are also grateful to their colleagues, Jiemin Zhu, Brett Handerson, Mark Timper and Dr. S. Elangovan, for their assistance in the experiments. This work was supported by the Gas Research Institute under Contract No. 5086-294-1292 and 5090-260-1985.

References

[1] J.B. Boyce, L.C. De Jonghe and R.A. Huggins, eds. in:Solid State Ionics-85 (North-Holland, Amsterdam, 1986).

[2] J.S. Newman, Electrochemical Systems (Prentice-Hall, Englewood Cliffs, NJ, 1973).

[3] M. Liu, B. Handerson and A. Joshi, Ext. Abstr. Electrochem. Soc. 90-2 (1990) 1088;
M. Liu and A. Joshi, in: ASM Engineered Materials Handbook, Vol. 4, Ceramics and Glass (1991) p. 1131.

[4] C. Milliken, D. Tucker, S. Elangovan and A. Khandkar, Ext. Abstr. No. 15, Electrochem. Soc. Montreal, Quebec, Canada, May 6–11, 1990.

[5] A. Khandkar, S. Elangovan, M. Liu and M. Timper, in: High Temperature Electrode Materials and Characterization, eds. D.D. Macdonald and A. Khandkar (Electrochem. Soc., PV 91-6, Pennington, NJ, 1991) pp. 175–190.

[6] S. Elangovan, A. Khandkar, M. Liu and M. Timper, in: High Temperature Electrode Materials and Characterization, eds. D.D. Macdonald and A. Khandkar (Electrochem. Soc., PV 91-6, Pennington, NJ, 1991) pp. 191–199.

[7] M. Liu, A. Khandkar and M. Timper, Proc. Natl. Fuel Cell Congr. (1990) pp. 527–531.

[8] M. Liu, J. Zhu, A. Virkar, A. Khandkar and A. Joshi, in: High Temperature Electrode Materials and Characterization, eds. D.D. Macdonald and A. Khandkar (Electrochem. Soc., PV 91-6, Pennington, NJ, 1991) pp. 137–157.

[9] A.J. Bard and L.R. Faulkner, Electrochemical Methods, Fundamentals and Applications (Wiley, New York, 1980).

[10] M. Liu and A. Khandkar, Ext. Abstr. Electrochem. Soc. 90 (1990) 1062.

[11] A. Virkar, J. Nachlas, A. Joshi and J. Diamond, J. Am. Ceram. Soc. 73 (1990) 3382.

[12] M. Liu, in: Ionic and Mixed Conducting Ceramics, eds. T.A. Ramanarayanan and H.L. Tuller (Electrochem. Soc., PV 91-12, Pennington, NJ, 1991) pp. 191–215.

[13] M. Liu, in: Ionic and Mixed Conducting Ceramics, eds. T.A. Ramanarayanan and H.L. Tuller (Electrochem. Soc., PV 91-12, Pennington, NJ, 1991) pp. 95–109.

[14] M. Liu and A. Joshi, in: Ionic and Mixed Conducting Ceramics, eds. T.A. Ramanarayanan and H.L. Tuller, (Electrochem. Soc., PV 91-12, Pennington, NJ, 1991) pp. 231–246.